Inorganica Chimica Acta 413 (2014) 187–193

Contents lists available at ScienceDirect

Inorganica Chimica Acta

journal homepage: www.elsevier.com/locate/ica

Construction of 1D to 3D cadmium(II) coordination polymers from 4-(imidazol-1-yl)-benzoic acid: Effect of bridging anions

Ying Feng, Da-Bin Wang, Bo Wan, Xin-Hua Li, Qian Shi *

Nanomaterials & Chemistry Key Laboratory, College of Chemistry and Materials Engineering, Wenzhou University, Wenzhou 325000, China

ARTICLE INFO

Article history:
Received 16 September 2013
Received in revised form 1 January 2014
Accepted 6 January 2014
Available online 23 January 2014

Keywords:
Cadmium(II) polymer
Anion-dependent effect
Crystal structure
Luminescence property

ABSTRACT

Three Cd(II) coordination polymers, $[Cd(IBA)Cl(H_2O)]_n$ (**1**), $[Cd(IBA)(CH_3COO)]_n$ (**2**) and $[Cd(IBA)N_3]_n$ (**3**) derived from HIBA (HIBA = 4-(imidazol-1-yl)-benzoic acid), have been designed and prepared in the existence of different anions. **1** is a 1D chain and consists of Cd_2Cl_2 units bridged by imidazolyl nitrogen atom and chelating carboxylate of IBA. In **2**, the adjacent Cd(II) are bridged by acetate to form a bis(carboxylate-O,O′)-Cd(II) dimeric unit, which is inter-connected by exo-tridentate IBA into a 2D layer, in which carboxylate of acetate and IBA alternatively bridge Cd(II) generating carboxylate-O,O′-Cd(II) chains. In **3**, $\mu_{1,1}$-azide bridges Cd(II) forming a helical chain, which is further inter-connected by exo-tridentate IBA into a two-folded interpenetrated 3D network with unusual **seh-3,5-$P4_32_12$** topology. These results show significant anion-dependent effect on the formation of network structures. Solid-state photoluminescence investigation at room temperature indicates complexes **1**–**3** emit the intense photoluminescence around 450 nm.

1. Introduction

The design and synthesis of metal–organic frameworks (MOFs) with unusual and tailorable structures are fundamental steps for the discovery and fabrication of various functional supramolecular devices or materials [1]. Molecular self-assembly based on the principle of crystal engineering has proven to be an efficient approach for the formation of 1D, 2D and 3D frameworks. The judicial selection of multifunctional organic ligands with different coordination sites linked by appropriate spacers is important for the design and construction of the desirable frameworks [2–4]. In the context, multidenate N,O-organic ligands containing nitrogen and carboxylate groups are excellent candidates to construct MOFs by closely controlling the properties of spacers, such as the length, shape, symmetry, flexibility and functionality [5]. For examples, Lin et al. have obtained a series of Cd(II) complexes, using ligands containing pyridyl and carboxylate groups [6]. Hong et al. reported a series of Ag(I), Cd(II) and Mn(II) MOFs with beautiful aesthetics and useful properties using aminobenzoic acids [5d–f]. However, the mechanism of molecular self-assembly is still unclear, the exact prediction and modification of target products are still difficult. The main reason is the assembly process of organic ligands and metal ions is also highly influenced by lots of other factors, such as coordination geometry of metal ions, counter anions, temperature, the solvent system and pH value of the solution [7]. Sometimes, a subtle alteration in any of these factors can result in new MOFs with different structural topologies and functions. Thus, understanding the factors that govern the assembly process is crucial to the development of MOFs. It is a common strategy to carry out a special study by only changing one of reaction conditions.

In the designed synthesis of MOFs, the imidazolyl unit is a promising building block owing to its ready availability and strong coordination ability [8–10]. Various MOFs were constructed from transition metal ions and organic ligands containing imidazolyl and carboxylate groups. In our study of imidazolyl-based functional materials, we are interested in 4-(imidazol-1-yl)-benzoic acid (HIBA) due to the non-linear property. It was known that the anion can not only balance the electron charge in the system, but also plays an important role on the coordination mode of the ligands in MOFs [11]. Recently, Co(II) [12] and Cd(II) [13–14] MOFs were constructed, but the anionic effect on the structures and properties have no been studied. In this work, we chose Cl^-, CH_3COO^-, and $N_3{}^-$ as the anions to construct the frameworks with IBA, and reported three Cd(II) coordination polymers, $[Cd(IBA)Cl(H_2O)]_n$ (**1**), $[Cd(IBA)(CH_3COO)]_n$ (**2**) and $[Cd(IBA)N_3]_n$ (**3**) (HIBA = 4-(imidazol-1-yl)-benzoic acid), in which the anions have an important effect on their structures and properties.

---

* Corresponding author. Tel.: +86 577 86596013; fax: +86 577 86596059.
E-mail address: shiq@wzu.edu.cn (Q. Shi).

http://dx.doi.org/10.1016/j.ica.2014.01.014

Table 1
Crystallographic data for the complexes.

	1	**2**	**3**
Molecular formula	$C_{10}H_9CdClN_2O_3$	$C_{12}H_{10}CdN_2O_4$	C_{10} $H_7CdN_5O_2$
Formula weight	353.04	358.62	341.61
T (K)	173(3)	173(3)	173(3)
Cryst color and form	yellow blocks	colorless blocks	pale yellow blocks
Cryst system	monoclinic	monoclinic	orthorhombic
space group	*C2/c*	*C2/c*	*Pbca*
a (Å)	19.487(7)	18.803(9)	15.967(6)
b (Å)	9.189(3)	8.128(4)	6.815(3)
c (Å)	12.856(5)	16.328(8)	20.113(8)
α (°)	90	90	90
β (°)	93.505(6)	103.930(5)	90
γ (°)	90	90	90
V (A^3)	2297.9(14)	2422(2)	2188.6(14)
Z	8	8	8
D_{calc} (Mg m^{-3})	2.041	1.967	2.074
F(000)	1376	1408	1328
θ_{max} (°)	27.48	27.46	27.49
Collected/unique	9382/2610	8904/2750	15842/2509
No. of parameters	164	174	164
Goodness-of-fit (GOF) on F^2	0.874	1.113	1.117
Final *R* indices [$I > 2\sigma(I)$][a,b]	$R_1 = 0.0217$	$R_1 = 0.0182$	$R_1 = 0.0228$
	$wR_2 = 0.0473$	$wR_2 = 0.0496$	$wR_2 = 0.0526$
R indices (all data)[a,b]	$R_1 = 0.0289$	$R_1 = 0.0212$	$R_1 = 0.0247$
	$wR_2 = 0.0487$	$wR_2 = 0.0514$	$wR_2 = 0.0537$
Largest peak and hole (e $Å^{-3}$)	0.540 and −0.432	0.772 and −0.548	0.970 and −0.480

[a] $R_1 = \sum ||F_o| - |F_c|| / \sum |F_o|$.
[b] $wR_2 = [\sum w(|F_o| - |F_c|)^2 / \sum w|F_o|^2]^{\frac{1}{2}}; w = [\sigma^2(F_o)^2 + (0.1(\max(F_o^2, 0) + 2F_c^2)/3)^2]^{-1}$.

Table 2
Selected bond lengths (Å) and Angles (°) for the complexes.[a]

Complex ***1***					
Cd(1)–O(1)	2.365(2)	Cd(1)–O(1A)	2.365(2)	Cd(1)–O(2)	2.3522(18)
Cd(1)–O(2A)	2.3522(18)	Cd(1)–Cl(1)	2.5500(9)	Cd(1)–Cl(1A)	2.5500(9)
Cd(2)–O(1W)	2.392(2)	Cd(2)–O(1WA)	2.392(2)	Cd(2)–N(1B)	2.233(2)
Cd(2)–N(1C)	2.233(2)	Cd(2)–Cl(1)	2.6796(9)	Cd(2)–Cl(1A)	2.6796(9)
O(2)–Cd(1)–O(1)	55.58(7)	O(2)–Cd(1)–O(1A)	119.83(7)	O(2)–Cd(1)–O(2A)	94.17(9)
O(1)–Cd(1)–Cl(1)	90.15(6)	O(1)–Cd(1)–Cl(1A)	93.73(5)	O(2)–Cd(1)–Cl(1)	94.42(6)
O(2)–Cd(1)–Cl(1A)	148.02(5)	N(1B)–Cd(2)–N(1C)	164.00(12)	N(1C)–Cd(2)–O(1W)	85.04(8)
N(1B)–Cd(2)–O(1W)	85.18(8)	O(1W)–Cd(2)–O(1WA)	104.49(11)	N(1B)–Cd(2)–Cl(1)	91.78(7)
N(1B)–Cd(2)–Cl(1A)	99.68(6)	O(1W)–Cd(2)–Cl(1)	83.64(6)	O(1WA)–Cd(2)–Cl(1)	170.95(6)
N(1B)–Cd(2)–Cl(1)	91.78(7)	N(1C)–Cd(2)–Cl(1)	99.68(6)	O(1W)–Cd(2)–Cl(1)	170.95(5)
O(1WA)–Cd(2)–Cl(1)	83.64(6)	Cl(1)–Cd(2)–Cl(1A)	88.56(4)		
Complex ***2***					
Cd(1)–O(2)	2.3261(15)	Cd(1)–O(2A)	2.3261(15)	Cd(1)–O(3)	2.3775(16)
Cd(1)–O(3A)	2.3775(16)	Cd(1)–N(1B)	2.2620(17)	Cd(1)–N(1C)	2.2620(17)
Cd(2)–O(1D)	2.2390(14)	Cd(2)–O(1AA)	2.2390(14)	Cd(2)–O(4)	2.2569(15)
Cd(2)–O(4A)	2.2569(15)				
N(1B)–Cd(1)–O(2)	91.54(5)	N(1C)–Cd(1)–O(2A)	91.54(5)	N(1B)–Cd(1)–O(2A)	98.64(5)
N(1C)–Cd(1)–O(2)	98.64(5)	N(1B)–Cd(1)–N(1C)	166.59(7)	O(2)–Cd(1)–O(2A)	81.44(8)
N(1B)–Cd(1)–O(3)	83.61(5)	N(1B)–Cd(1)–O(3A)	86.35(5)	N(1C)–Cd(1)–O(3)	86.35(5)
N(1C)–Cd(1)–O(3A)	83.61(5)	O(2)–Cd(1)–O(3)	97.79(7)	O(2)–Cd(1)–O(3A)	177.62(4)
O(2A)–Cd(1)–O(3)	177.62(4)	O(2A)–Cd(1)–O(3A)	97.79(7)	O(3)–Cd(1)–O(3A)	83.08(9)
O(1D)–Cd(2)–O(4)	91.94(6)	O(1AA)–Cd(2)–O(4A)	91.94(6)	O(1AA)–Cd(2)–O(4)	98.93(6)
O(1D)–Cd(2)–O(4A)	98.93(6)	O(4)–Cd(2)–O(4A)	144.96(7)	O(1AA)–Cd(2)–O(1D)	143.38(7)
Complex ***3***					
Cd(1)–O(1A)	2.2933(18)	Cd(1)–N(1)	2.233(2)	Cd1–O(2B)	2.2848(17)
Cd1–N(3)	2.255(2)	Cd1–N(3C)	2.247(2)		
N(1)–Cd(1)–N(3)	120.10(8)	N(1)–Cd(1)–N(3C)	110.56(7)	N(3)–Cd(1)–N(3C)	129.29(3)
N(1)–Cd(1)–O(2B)	87.23(7)	N(3)–Cd(1)–O(2B)	88.44(7)	N(3C)–Cd(1)–O(2B)	96.40(8)
N(1)–Cd(1)–O(1A)	91.25(7)	N(3)–Cd(1)–O(1A)	91.67(8)	N(3C)–Cd(1)–O(1A)	85.36(7)
O(2B)–Cd(1)–O(1A)	171.81(7)				

[a] Symmetry operations. For **1:** (A) $-x+1, y, -z+3/2$ (B) $x-1/2, -y+3/2, z+1/2$ (C) $-x+3/2, y+3/2, -z+1$; For **2**: (A) $x-1/2, -y+3/2, z-1/2$ (B) $x+3/2, -y+3/2, -z+2$ (C) $-x+1, y, -z+3/2$ (D) $-x+1, y-1, -z+3/2$ (AA) $x, y-1, z$; For **3**: (A) $-x+2, y+1/2, -z+3/2$ (B) $x+1/2, -y+1/2, -z+1$, (C) $-x+3/2, -y, z+1/2$.

2. Experimental

2.1. Materials and physical measurements

All chemicals were purchased and used as received. Elemental analyses were performed with a Thermo 1112 elemental analyzer. IR spectra were measured from KBr pellets on a Bruker-Tensor 27FT-IR spectrometer. Photoluminescence spectra were recorded on a Thermo Aminco-Bowan2 spectrometer with 450-W xenon lamp monochromatized by double grating (1200 gr/mu) at room temperature. Thermal stability studies were carried out on a NETSCHZ STA 449C thermoanalyzer under N_2 at a heating rate of 10 °C min^{-1}.

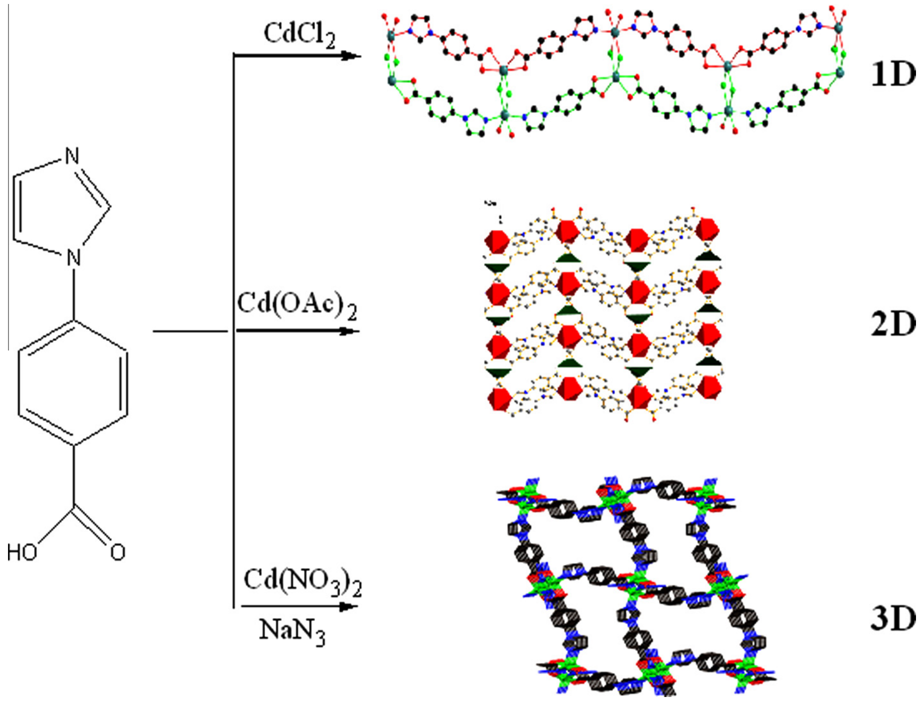

Scheme 1. Schematic drawing of the reactions between HIBA and Cd(II) salts.

2.2. Synthesis of [Cd(IBA)Cl(H_2O)]$_n$ (*1*)

A mixture of $CdCl_2·2.5H_2O$ (0.143 g, 0.6 mmol), HIBA (0.0376 g, 0.2 mmol) and H_2O (15 ml) was sealed in a 30 ml Teflon-lined autoclave and heating to 120 °C for 3 days, followed by slow cooling (10 °C h^{-1}) to room temperature during 24 h. The yellow block crystals were obtained (yield: 51%). *Anal.* Calc. for $C_{10}H_9CdClN_2O_3$: C, 34.02; H, 2.57; N, 7.93. Found: C, 34.13; H, 2.52; N, 7.98%.

2.3. Synthesis of [Cd(IBA)(CH_3COO)]$_n$ (*2*)

The colorless crystals of **2** were formed using $Cd(OAc)_2·2H_2O$ (0.160 g, 0.6 mmol) instead of $CdCl_2·2.5H_2O$ in the same reaction conditions as described above (yield: 78.8%). *Anal.* Calc. for $C_{12}H_{10}CdN_2O_4$: C, 40.19; H, 2.81; N, 7.81. Found: C, 40.18; H, 2.70; N, 7.87%.

2.4. Synthesis of [Cd(IBA)N_3]$_n$ (*3*)

The pale yellow block crystals of **3** were obtained using $Cd(NO_3)_2·4H_2O$ (0.185 g, 0.6 mmol) and NaN_3 (0.013 g, 0.2 mmol) instead of $CdCl_2·2.5H_2O$ in the same reaction conditions as described above (yield: 73%). *Anal.* Calc. for $C_{10}H_7CdN_5O_2$: C, 35.16; H, 1.81; N, 20.38. Found: C, 35.16; H, 1.95; N, 20.50%.

2.5. X-ray crystallography

Crystal and intensity data were collected on a Bruker Smart APEX II CCD diffractometer with graphite-monochromated Mo Kα radiation (λ = 0.71073 Å) at 173 K. Empirical absorption corrections were applied using the SADABS program. The structures were solved by direct methods and refined by the full-matrix least-squares based on F^2 using SHELXTL-97 program. Crystal data as well as details of data collection and refinement for the complexes are summarized in Table 1. Selected bond lengths and angles are listed in Table 2.

3. Results and discussion

3.1. Preparation

Solvothermal reaction is preference to the other methods in this system because of the poor solubility of HIBA in water and most common organic solvents. A series of experiments were carried out in order to get the suitable reaction temperature. It has been found that the best temperature for the crystal growth of the Cd(II) complexes is at 120 °C in the mixed solvent. In the reaction of Cd(II) salts and HIBA, one-dimensional complex **1** and two-dimensional complex **2** were formed in the existence of Cl^- or CH_3COO^-. When the anion is NO_3^- and N_3^-, N_3^- participates in coordination instead of NO_3^-, forming an three-dimensional complex **3** (Scheme 1). The result indicates that anions have an important effect on the structure of complexes.

The IR spectrum of complex **1** shows typical antisymmetric $\nu_{asym}(CO_2)$ and symmetric $\nu_{sym}(CO_2)$ stretching bands of carboxylate group at 1523 and 1406 cm^{-1}, respectively. The separation between $\nu_{asym}(CO_2)$ and $\nu_{sym}(CO_2)$ is 117 cm^{-1}, indicating a chelating coordination mode of carboxylate group [5d]. However, the characteristic bands of the carboxylate group of IBA are shown at 1545 and 1397 cm^{-1} for **2**, at 1544 and 1400 cm^{-1} for **3**. The separations (Δ) between ν_{asym} (CO_2) and $\nu_{sym}(CO_2)$ are 148 and 144 cm^{-1}, respectively, suggesting a μ_2-carboxylate bridging mode. The presence of a sharp peak of 2071 cm^{-1} in IR spectrum of **3** shows that the azide anion adopts a μ_2-1,1-bridging mode.

In complex **1**, Cd(1) is in a six-coordinated mode and is bonded by two cis-coordinated Cl^- and four oxygen atoms from the chelating carboxylate of different IBA. Cd(2) is coordinated by two trans-coordinated imidazolyl nitrogen atoms, two water molecules and two cis-coordinated Cl^- in a distorted octahedral geometry (Fig. 1a). The Cd···Cd distance bridged by IBA is 12.363 Å. The twisting angle between imidazoly ring and phenyl ring is 11.6°, while the twisting angle between phenyl ring and $-CO_2^-$ is 6.8°. Cl^- acts as a μ_2-bridge between different Cd(II) to form a Cd_2Cl_2 building unit. The separation of Cd···Cd is 3.651 Å. IBA connect Cd_2Cl_2 units

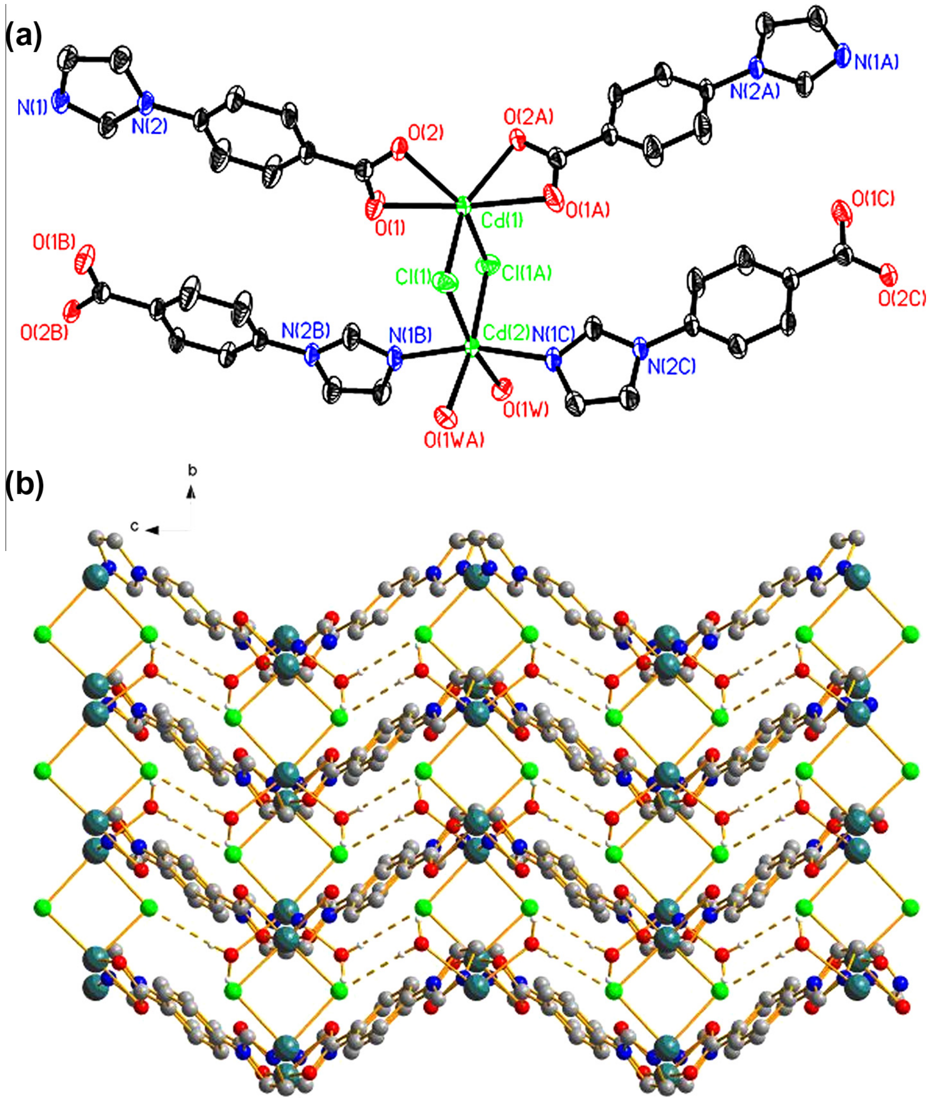

Fig. 1. (a) ORTEP view of the Cd(II) coordination environments in **1** (30% probability ellipsoids). (b) Perspective view of 3D hydrogen bonding network in **1**.

into a 1D chain consisting of rectangular grids (Scheme 1). It should be noted that the water ligands form strong hydrogen bonds with carboxylate oxygen atoms of IBA [O1W–H1W···O2^{i} 2.749 Å, symmetry code: (i) $-x+1$, $y-1$, $-z+3/2$]. The hydrogen bonding interactions further extend 1D chains into a 2D network, which is further extended into a 3D network by the hydrogen bonding interactions between water and Cl^{-} [O1W–H2W···Cl1^{ii} 3.449 Å, symmetry code: (ii) x, $-y+1$, $z+1/2$]. (Fig. 1b).

Complex **2** is a 2D coordination polymer based on bicarboxylate-O,O′-bridged Cd(II) chains. Cd(1) is in a distorted octahedral geometry and is coordinated by four carboxylate oxygen atoms from two IBA and two acetate, respectively, and two nitrogen atoms from different IBA (Fig. 2a). Four carboxylate oxygen atoms comprise the equatorial plane and Cd(1) is coplanar with their mean plane, two imidazolyl nitrogen atoms occupy the axial positions with the N–Cd–N bond angle of 166.59(7)°. The bond angles between the *cis* donors around Cd(1) range from 81.44(8)° to 98.93(6)°. The Cd(1)–N bond length of 2.2620(17) Å is slightly shorter than that of Cd(1)–O bond length of 2.3261(15) and 2.3775(16) Å, suggesting a compressed octahedron. Cd(2) is a distorted tetrahedral geometry and is coordinated by four carboxylate oxygen atoms from two IBA and two acetate. Cd(2)–O bond distances of 2.2390(14) and 2.2569(15) Å are shorter than those of Cd(1)–O. Acetate serves as a μ_2,η^2-carboxylate bridge. Two acetate bridge Cd(1) and Cd(2) forming a dicarboxylate-Cd(II) eight-membered ring with Cd···Cd distance of 4.037 Å. Different from that in **1**, IBA adopts an *exo*-tridentate bridging mode through imidazolyl nitrogen atom and μ_2,η^2-carboxylate group (Scheme 1b). The imidazolyl ring is slightly distorted with respect to the phenyl ring with the dihedral angle between them being 9.5°, while the twisting angle between phenyl ring and $-CO_2^{-}$ is 19.8°, which are much different from those in **1**. Each pair of adjacent Cd(1) and Cd(2) is alternatively bridged by carboxylate-O,O′ of acetate and IBA to generate an infinite Cd(II)-carboxylate chain (Fig. 2b). The chain is inter-connected by IBA into a 2D network (Scheme 1). There are no other short contacts or noteworthy aryl-aryl interactions between the adjacent 2D layers.

In complex **3**, the asymmetric unit contains one Cd(II), one IBA and one azide. As shown in Fig. 3a, Cd(II) is in a distorted trigonal–bipyramidal geometry with $\tau = 0.71$ [15]. The equatorial plane comprises two azide nitrogen atoms [N(3) and N(3C)] and one imidazolyl nitrogen atom (N1). Two carboxylate oxygen atoms [O(1A) and O(2B)] from different IBA occupy the axial positions with O(1A)–Cd(1)–O(2B) bond angle of 171.81(7)°. IBA adopts an *exo*-tridentate bridging mode (Scheme 1b). The dihedral angle between imidazoly ring and phenyl ring is 30.8°, which is larger than that in **1** and **2**, while the twisting angle between phenyl ring and $-CO_2^{-}$ is 4.0°. $\mu_{1,1}$-Azide connects Cd(II) into a helical chain

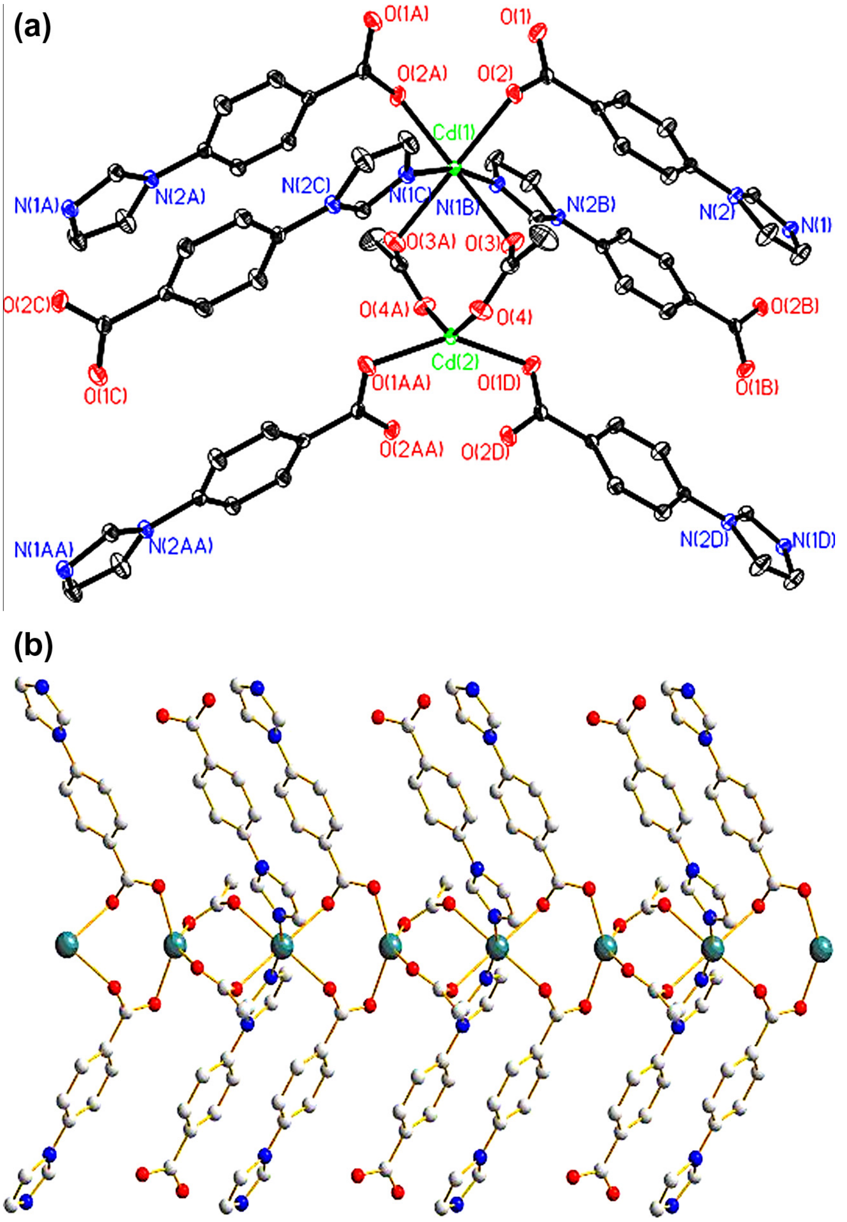

Fig. 2. (a) ORTEP view of the Cd(II) coordination environments in **1** (30% probability ellipsoids). (b) Perspective view of the Cd(II)-carboxylate chain in **2**.

(Fig. 3b), in which the adjacent Cd(II) are further bridged by μ_{2},η^{2}-carboxylate of IBA through the formation a (Cd–N–Cd–O–C–O) six-membered ring. IBA further extend the chain into a 3D network (Scheme 1). However, because of the absence of larger guest molecules to fill the larger void space, the potential voids are filled via mutual interpenetration to generate a twofold interpenetrating architecture. Topologically, in **3**, the Cd(II) center can be simplified as a 5-connected node, while IBA connecting three Cd(II) can be regarded as a 3-connected node. Therefore the whole framework **3** can be designated as a twofold interpenetrating (3,5)-connected **seh-3,5-*P*4$_3$2$_1$2** topology with point symbol $(37^{2})(3^{2}7^{5}8^{3})$ and long vertex symbol (3.7.7)(3.3.7.7.7.7.7.8.8.8$_2$) [16] (Fig. 3c). Comparing with (3,4)- and (3,6)-connected nets, (3,5)-connected nets are not commonly observed in coordination polymers. Moreover, for known (3,5)-connected nets, the framework with **gra** and **hms** topologies have been well investigated [17], however, **seh-3,5-*P*4$_3$2$_1$2** topology is observed only in very few compounds [18].

Fluorescence spectra were performed on at room temperature. In complexes **1**–**3**, strong blue fluorescence at 450 nm was observed upon the excitation at 370 nm (Fig. 4). To understand the nature of the emission band, the photoluminescence of HIBA was also determined. While the HIBA ligand displays fluorescence at 440 nm. Although the maximum emission wavelengths of complexes **1**–**3** undergo a slight blue-shift, the emission bands for complexes **1**–**3** are very similar to that found for the free ligand in terms of position and band shape. Therefore, the emission bands of complexes **1**–**3** are mainly due to an intraligand emission state as reported for Cd(II) or other d^{10} metal complexes with N-donor ligands. The enhancement of luminescence in the complex **1** is, perhaps, may be attributed to the rigidity of **1**. This rigidity is favor of energy transfer and reduces the loss of energy through a radiationless pathway [19,20].

Thermogravimetric analyses (TGA) of complexes **1**–**3** were performed on polycrystalline samples in a nitrogen atmosphere

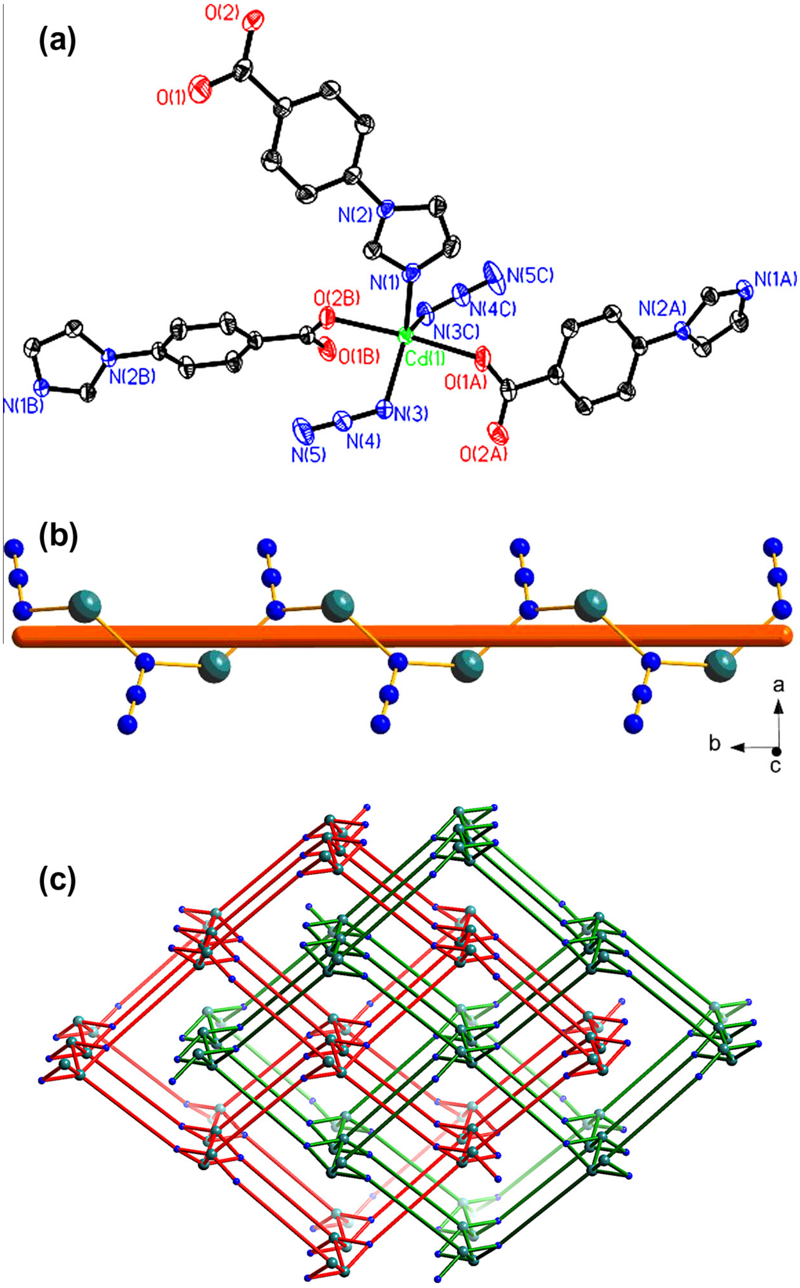

Fig. 3. (a) ORTEP view of the Cd(II) coordination environments in **3** (30% probability ellipsoids). (b) Perspective view of the Cd-N_{N3} helical chain in **3**. (c) Twofold interpenetrating network in 3.

(Supporting information, Fig. S1). For **1**, the weight loss of 12.2% from 156 to 180 °C corresponds to the loss of coordination water molecule and Cl⁻ (calcd: 11.5%), subsequent decomposition occurs after 365 °C. However, **2** and **3** are stabled up to 370 and 390 °C, respectively.

4. Conclusion

Three cadmium(II) coordination polymers based on IBA and bridging anions (Cl, CH_3COO^-, N_3^-) have been synthesized and structurally characterized. In **1,** IBA bridges two Cd(II) through its imidazolyl nitrogen atom and chelating carboxylate group. IBA and Cl⁻ link Cd(II) into a 1D chain, which is further extended into a 3D network by hydrogen bonding interactions. IBA in **2** and **3** adopts an *exo*-tridentate bridging mode through imidazolyl nitrogen atom and $\mu_{2,}\eta^2$-carboxylate group. In **2,** IBA and

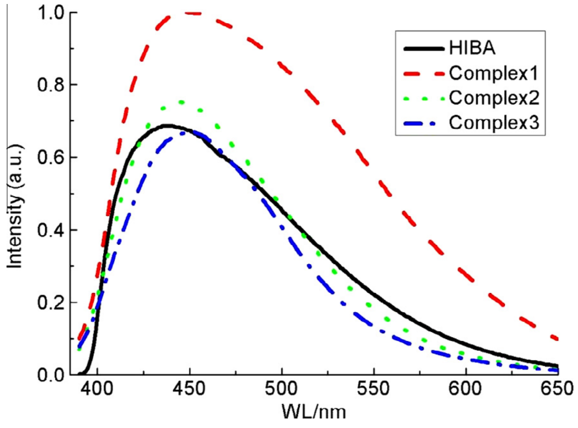

Fig. 4. The solid emission spectra of free HIBA ligand and complexes **1–3** at room temperature.

μ_2,η^2-acetate link Cd(II) into a 2D layer consisting of carboxylate-Cd(II) chains alternatively bridged by carboxylate of acetate and IBA. However, IBA and $\mu_{1,1}$-azide in **3** link Cd(II) into a two-folded interpenetrating 3D network consisting of N_{N3}–Cd(II) helical chains. The maximum fluorescence peaks of the complexes are somewhat blue-shift campared to that of the free ligand. The fluorescence intensity of the complexes is weakened from 1D to 3D network. In summary, this research demonstrates the bridging anions have an important effect on assembly of functional ligands containing imidazolyl and carboxylate with metal ions. Novel supramolecular architectures owning different structures can be constructed using this strategy.

Acknowledgments

We thank the National Natural Science Foundation of China (20971101 and 21271142) for financial support of this study. Helpful discussions with Prof. Ruihu Wang (Fujian Institute of Research on the Structure of Matter, Chinese Academy of Sciences) are also acknowledged.

Appendix A. Supplementary material

CCDC 816070, 816069 and 794750 contains the supplementary crystallographic data for **1**–**3**. These data can be obtained free of charge from The Cambridge Crystallographic Data Centre via www.ccdc.cam.ac.uk/data_request/cif. Supplementary data associated with this article can be found, in the online version, at http://dx.doi.org/10.1016/j.ica.2014.01.014.

References

[1] (a) D. Bradshaw, J.B. Claridge, E.J. Cussen, T.J. Prior, M.J. Rosseinsky, Acc. Chem. Res. 38 (2005) 273;
(b) J.M. Rueff, J.F. Nierengarten, P. Gilliot, A. Demessence, O. Cregut, M. Drillon, P. Rabu, Chem. Mater. 16 (2004) 2933;
(c) L. Pan, D.H. Olson, L.R.R. Ciemnolonski, Li, J. Angew. Chem., Int. Ed. 45 (2006) 616;
(d) C.Y. Su, Y.P. Cai, C.L. Chen, M.D. Smith, W. Kaim, H.C.Z. Loye, J. Am. Chem. Soc. 125 (2003) 8595;
(e) Y.B. Dong, Y.Y. Jiang, J. Li, J.P. Ma, F.L. Liu, B. Tang, R.Q. Huang, S.R. Batten, J. Am. Chem. Soc. 129 (2007) 4520.
[2] J. Makarevic, M. Jokic, B. Peric, V. Tomisic, B. Kojic-Prodic, M. Zinic, Chem. Eur. J. 7 (2001) 3328.
[3] E.Q. Gao, Y.F. Yue, S.Q. Bai, Z. He, C.H. Yan, J. Am. Chem. Soc. 126 (2004) 1419.
[4] S.B. Ren, X.L. Yang, J. Zhang, Y.Z. Li, Y.X. Zheng, H.B. Du, X.Z. You, CrystEngComm 11 (2009) 246.
[5] (a) M.H. Zeng, B. Wang, X.Y. Wang, W.X. Zhang, X.M. Chen, S. Gao, Inorg. Chem. 45 (2006) 7069;
(b) B. Ding, Y.Y. Liu, Y.Q. Huang, W. Shi, P. Cheng, D.Z. Liao, S.P. Yan, Cryst. Growth Des. 9 (2009) 593;
(c) X. Li, X. Wang, S. Gao, R. Cao, Inorg. Chem. 45 (2006) 1508;
(d) R. Wang, M. Hong, J. Luo, R. Cao, Q. Shi. J. Weng, Eur. J. Inorg. Chem. (2002) 2904.;
(e) R. Wang, E. Gao, M. Hong, S. Gao, J. Luo, Z. Lin, L. Han, R. Cao, Inorg. Chem. 42 (2003) 5486;
(f) R. Wang, M. Hong, J. Luo, F. Jiang, L. Han, Z. Lin, R. Cao, Inorg. Chim. Acta 357 (2004) 103.
[6] O.R. Evans, W.B. Lin, Acc. Chem. Res. 35 (2002) 511.
[7] (a) X. Zhu, H.Y. Ge, Y.M. Zhang, B.L. Li, Y. Zhang, Polyhedron 25 (2006) 1875;
(b) X.R. Meng, Y.L. Song, H.W. Hou, H.Y. Han, B. Xiao, Y.T. Fan, Y. Zhu, Inorg. Chem. 43 (2004) 3528;
(c) M. Du, X.H. Bu, Y.M. Guo, H. Liu, S.R. Batten, J. Ribas, T.C.W. Mak, Inorg. Chem. 41 (2002) 4904;
(d) Z.G. Guo, R. Cao, X.J. Li, D.Q. Yuan, W.H. Bi, X.D. Zhu, Y.F. Li, Eur. J. Inorg. Chem. (2007) 742;
(e) J. Tao, X.M. Chen, R.B. Huang, L.S. Zheng, J. Solid State Chem. 170 (2003) 130.
[8] (a) H. He, D. Collins, F. Dai, X. Zhao, G. Zhang, H. Ma, D. Sun, Cryst. Growth Des. 10 (2010) 895;
(b) C.Y. Sun, X.J. Zheng, S. Gao, L.C. Li, L.P. Jin, Eur. J. Inorg. Chem. (2005) 4150;
(c) H.P. Jia, W. Li, Z.F. Ju, J. Zhang, Inorg. Chem. Commun. (2007) 397;
(d) M.H. Zeng, M.X. Yao, H. Liang, W.X. Zhang, X.M. Chen, Angew. Chem., Int. Ed. 46 (2007) 1832;
(e) X. Li, X. Weng, R. Tang, Y. Lin, Z. Ke, W. Zhou, R. Cao, Cryst. Growth Des. 10 (2010) 3228.
[9] Z.S. Bai, S.S. Chen, Z.H. Zhang, M.S. Chen, G.X. Liu, W.Y. Sun, Sci. China B 52 (2009) 459.
[10] F. Li, J.Y. Zheng, Y.M. Dai, J.F. Huang, X.Q. Wang, Chinese J. Struct. Chem. 29 (2010) 839.
[11] (a) Q. Shi, Y.T. Sun, L.Z. Sheng, K.F. Ma, M.L. Hu, X.G. Hu, S.M. Huang, Cryst. Growth Des. 8 (2008) 3401;
(b) Q. Shi, L.J. Xu, J.X. Ji, Y.M. Li, R.H. Wang, Z.Y. Zhou, R. Cao, M.C. Hong, A.S.C. Chan, Inorg. Chem. Commun. 7 (2004) 1254;
(c) K.I. Naettinen, P.E.N. de Bairos, P.J. Seppaelae, K.T. Rissanen, Eur. J. Inorg. Chem. 14 (2005) 2819;
(d) X. Li, J. Illigen, M. Nieger, S. Michel, C.A. Schalley, Chem. Eur. J. 9 (2003) 1332;
(e) C.A. Schalley, G. Silva, C.F. Nising, P. Linnartz, Helv. Chim. Acta 85 (2002) 1578;
(f) Z. Zheng, C.B. Knobler, M.F. Hawthorne, J. Am. Chem. Soc. 117 (1995) 5105;
(g) P.A. R.aital, M. Mikuriya, D. Ray, Eur. J. Inorg. Chem. 34 (2007) 5360.
[12] J.Z. Zhang, W.R. Cao, J.X. Pan, Q.W. Chen, Inorg. Chem. Commun. 10 (2007) 1360.
[13] A. Aijaz, E. Barea, P.K. Bharadwaj, Cryst. Growth Des. 9 (2009) 4480.
[14] X.D. Chen, X.H. Zhao, M. Chen, M. Du, Chem. Eur. J. 15 (2009) 12974.
[15] A.W. Addison, T.N. Rao, J. Reedijk, J. van Rijn, G.C. Verschoor, J. Chem. Soc., Dalton Trans. (1984) 1349.
[16] V.A. Blatov, A. P. Shevchenko, D.M. Proserpio, Topos 4.0, 2007.
[17] (a) C. Gao, S. Liu, L. Xie, Y. Ren, J. Cao, C. Sun, CrystEngComm 9 (2007) 545;
(b) L. Hou, J.-P. Zhang, X.-M. Chen, Cryst. Growth Des. 9 (2009) 2415;
(c) Z.-B. Han, Y.-F. Liang, M. Zhou, Y.-R. Zhang, L. Li, J. Tong, CrystEngComm 14 (2012) 6952;
(d) H. He, F. Dai, D. Sun, Dalton Trans. (2009) 763;
(e) Du Li-Yun, Wen-Juan Shi, Lei Hou, Yao-Yu Wang, Qi-Zhen Shi, Zhonghua Zhu, Inorg. Chem. 52 (2013) 14018.
[18] (a) J. Zhang, S. Chen, A. Zingiryan, X. Bu, J. Am. Chem. Soc. 130 (2008) 17246;
(b) W. Li, H.-P. Jia, Z.-F. Ju, J. Zhang, Cryst. Growth Des. 6 (2006) 2136;
(c) S.R. Miller, E. Lear, J. Gonzalez, A.M.Z. Slawin, P.A. Wright, N. Guillou, G. Férey, Dalton Trans. 20 (2005) 3319;
(d) F.-C. Liu, Y.-F. Zeng, J.-P. Zhao, B.-W. Hu, E.C. Sañudo, J. Ribas, X.-H. Bu, Inorg. Chem. 46 (2007) 7698.
[19] J. Lu, K. Zhao, Q.R. Fang, J.Q. Xu, J.H. Yu, X. Zhang, H.Y. Bie, T.G. Wang, Cryst. Growth Des. 5 (2005) 1091.
[20] L.L. Wen, D.B. Dang, C.Y. Duan, Y.Z. Li, Z.F. Tian, Q.J. Meng, Inorg. Chem. 44 (2005) 7161.